Journal of Crystal Growth 449 (2016) 62–66

Contents lists available at ScienceDirect

Journal of Crystal Growth

journal homepage: www.elsevier.com/locate/jcrysgro

Structure and magnetic properties of spinel-perovskite nanocomposite thin films on $SrTiO_3$ (111) substrates

Dong Hun Kim *, Junho Yang, Min Seok Kim, Tae Cheol Kim

Department of Materials Science and Engineering, Myongji University, Yongin 17058, Republic of Korea

ARTICLE INFO

Article history:
Received 23 February 2016
Accepted 26 May 2016
Communicated by: David Norton
Available online 27 May 2016

Keywords:
A1. Crystal structure
A1. Nanostructures
A3. Laser epitaxy
B1. Perovskites
B2. Ferroelectric materials
B2. Magnetic materials

ABSTRACT

Epitaxial $CoFe_2O_4$–$BiFeO_3$ nanocomposite thin films were synthesized on perovskite structured $SrTiO_3$ (001) and (111) substrates by combinatorial pulsed laser deposition and characterized using scanning electron microscopy, x-ray diffraction, and vibrating sample magnetometer. Triangular $BiFeO_3$ nanopillars were formed in a $CoFe_2O_4$ matrix on (111) oriented $SrTiO_3$ substrates, while $CoFe_2O_4$ nanopillars with rectangular or square top surfaces grew in a $BiFeO_3$ matrix on (001) substrates. The magnetic hysteresis loops of nanocomposites on (111) oriented $SrTiO_3$ substrates showed isotropic properties due to the strain relaxation while those of films on $SrTiO_3$ (001) substrates exhibited a strong out-of-plane anisotropy originated from shape and strain effects.

1. Introduction

In recent years, considerable attention has been paid to multiferroic nanocomposites composed of immiscible ferromagnetic and ferroelectric phases for sensors, actuators, or new types of electronic memory devices due to their potential in applications [1–4]. Multiferroics exhibit two or more of ferroic properties in a single material but most single-phase multiferroic materials have reported to have a low magnetoelectric coupling occurring at low temperature which limits the device application. Recent interest in multiferroics has been concentrated on the nanocomposites possessing both ferroelectric and ferromagnetic properties with magnetoelectric coupling.

When the spinel structured magnetic cobalt ferrite ($CoFe_2O_4$, CFO) and perovskite structured ferroelectric bismuth ferrite ($BiFeO_3$, BFO) phases are deposited by pulsed laser deposition (PLD) or sputter simultaneously from a single composite target or two targets of BFO and CFO on single crystal substrates, two-phase multiferroic nanocomposite thin films grow spontaneously which called self-assembled nanocomposites instead of forming solid solution [5–8].

To date, self-assembled CFO–BFO nanocomposites have been exclusively grown on (001) oriented single crystal perovskite substrates. A ferrimagnetic CFO grows epitaxially as pillars along the [001] direction within an immiscible ferroelectric perovskite BFO on (001) substrates. This nanocomposite is very promising for high density memory applications that require a strong magnetic anisotropy with a magnetic easy axis either normal or parallel to the substrate. Owing to the shape of the magnetic CFO pillar and strain effects, CFO–BFO nanocomposites on (001) substrate have a strong magnetic anisotropy with a preferred axis of magnetization oriented perpendicular to the substrate. The epitaxy of CFO in the BFO matrix along the vertical interface creates new strain in the out-of-plane direction leading the magnetoelastic anisotropy originated from the compressive CFO in addition to the in-plane strain constrained from the substrates [9–12].

The magnetic and ferroelectric properties of the CFO–BFO nanocomposites strongly depend not only on the strain states of both the phases, but also the growth orientation. It has been reported that the structure of a CFO–BFO nanocomposite on (111) oriented $SrTiO_3$ (STO) substrate showed a totally different morphology from that of nanocomposite on STO (001) substrate [1,10,13–15]. The triangular shaped $BiFeO_3$ nanopillars embedded in a CFO matrix and it was confirmed by magnetic force microcopy (MFM) [14,15].

We have previously reported that CFO–BFO nanocomposites with different CFO and BFO ratios grown on STO (001) substrates showed different morphologies and magnetic anisotropy. The composition gradient was achieved by combinatorial PLD (CPLD). The CFO and BFO ratios required to form a well-defined nanostructure on STO (001) and (111) substrate is different because the matrix and nanopillars are changed on each substrate. In this paper, we report on the growth of CFO–BFO nanocomposites by CPLD on $SrTiO_3$ (111) substrates with a focus on investigating microstructure and magnetic properties. We compare the structure of the nanocomposites grown by CPLD on (001) and (111) oriented

* Corresponding author.
E-mail address: dhkim@mju.ac.kr (D.H. Kim).

http://dx.doi.org/10.1016/j.jcrysgro.2016.05.041
0022-0248/

substrates and go on to investigate the relationship between the magnetic properties and structure or BFO/CFO ratio.

2. Experimental methods

CFO ($a_{bulk,CFO}$=8.392 Å, JCPDS # 22-1086) target was prepared by a conventional oxide sintering method. A mixture of CoO (purity, 99.9%) and Fe_2O_3 (purity, 99.5%) was calcined at 1100 °C after ball milling for 24 h. Disk-shaped 1 in. diameter CFO pellet then sintered at 1300 °C in the box furnace for 5 h. A commercial Bi-rich $Bi_{1.2}FeO_3$ target was prepared ($a_{bulk,\ BFO}$=3.965 Å, Plasmaterials, CA).

Epitaxial CFO–BFO nanocomposite thin films were grown on (111) oriented STO substrates by PLD at 650 °C of substrate temperature. The bulk lattice parameter of the commercial substrate was $a_{bulk,\ STO}$=3.905 Å (JCPDS # 35-0734). The BFO and CFO targets were ablated with a KrF excimer laser (λ=248 nm) at 5 mTorr oxygen pressure. The laser hit the targets with 2.6 J/cm^2 of the fluence and 10 Hz of frequency. For comparison, CFO–BFO nanocomposites were prepared under the same deposition condition on (001) oriented STO substrate.

CPLD was applied to optimize the deposition condition to obtain well-defined nanocomposites and to produce samples in a wide range composition. The nanocomposite thin films were obtained by alternative ablation of the first target (CFO) at 0° and the second target (BFO) at 180° without substrate rotation during deposition to vary the thickness and composition gradients as a function of substrate position. Five 5 mm × 5mm sized STO (111) substrates were lined up in a row. The rotation axis of the substrate is 18 mm offset against the target center and alternative ablating of two targets was repeated until getting desired thickness, typically 100 nm of a center sample. The number of laser ablations on the CFO and BFO targets were 250 and 100 times, respectively, and this process repeated 200 times.

The crystal structure and the interplanar spacing of the BFO and CFO phases in the nanocomposite thin films were determined by XRD (X-ray diffraction, PANalytical X'Pert Pro, λ=1.5406 Å). The surface morphology of the nanocomposites was observed by scanning electron microscopy (SEM, Helios Nanolab 600). Some of the samples were etched in 10% diluted hydrochloric acid (HCl) to remove BFO instead of getting rid of CFO to investigate the growth mode of nanocomposite on STO (111) substrate.

In-plane and out-of-plane magnetic hysteresis loops were measured using vibrating sample magnetometry (VSM, ADE model 1660) at room temperature. Magnetic field ranging from −10 kOe to 10 kOe was applied along the parallel and perpendicular directions with respect to the substrate. The magnetization was estimated for whole films instead of normalizing for the volume of the magnetic CFO.

3. Results and discussion

Five samples with different CFO and BFO contents were grown in the same chamber with a CPLD method using end BFO and CFO targets. It has been proved that CPLD is a very powerful thin film growth technique to produce wide range composition films with a linear composition gradient as a function of distance [12,16,17]. The composition spread nanocomposite thin films can be obtained with two end targets and a single step deposition instead of making individual target and growing respective film. Especially, CPLD is very useful for studying nanocomposite growth whose structure varies dramatically according to the composition change.

The surface morphology of CFO–BFO nanocomposites on (111) oriented STO substrates grown by CPLD are shown in Fig. 1(a)-1–(e)-1. Nanocomposites on STO (001) substrates grown with the same deposition conditions are compared in Fig. 1(a)-2–(e)-2. The samples with the same column have the same CFO and BFO ratio. The ablation numbers and sample positions were fixed at each deposition which explained below.

At the spinel-rich end of the nanocomposite on STO (111) substrate shown in Fig. 1(a)-1, the bright triangular and hexagonal phases with about 100 nm side length are randomly distributed. As the BFO content increases, the size of these triangular nanopillars increases by merging with neighboring pillars forming relatively irregular shapes. From the contrast comparison of series samples (Fig. 1(a)-1–(e)-1) it is concluded that the triangular phase and a matrix correspond to the BFO and CFO under complete phase separation assumption. For a BFO rich nanocomposite (Fig. 1 (e)-1), most parts of films are covered by BFO phase and a very small portion of dark CFO is observed.

The observed matrix and the nanostructured phases are totally opposite to those of nanocomposites on (001) substrates which a rectangle top view CFO grows as a pillar in a BFO matrix (Fig. 1(a)-2–(e)-2). The rectangular CFO with sides of length ~20 −50 nm grew along the [110] direction of the STO substrates. The nanopillar size is much smaller than that of nanocomposite on (111)

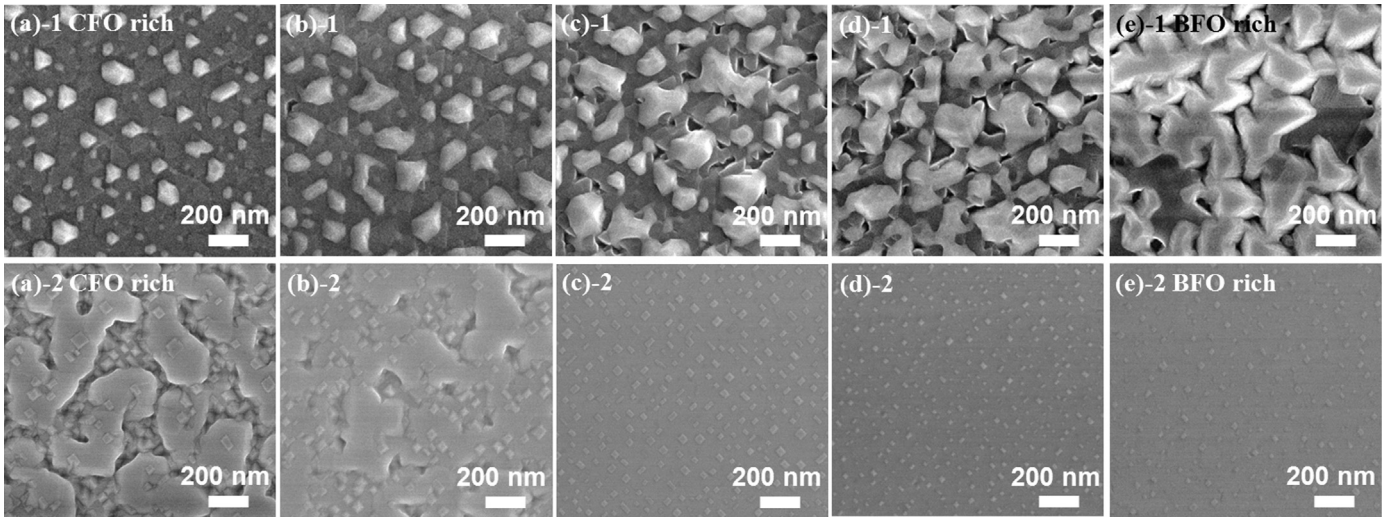

Fig. 1. (a)-1–(e)-1 Top view SEM images of CFO–BFO nanocomposites on STO (111) substrates fabricated at 650 °C under 5 mTorr of oxygen by CPLD. (a)-2–(e)-2 Top view SEM images of CFO–BFO nanocomposites on STO (001) substrates grown under the same deposition condition. BFO contents increase from (a)–(e).